18th International Conference
ENGINEERING MECHANICS 2012
Svratka, Czech Republic, May 14 – 17, 2012

pp. 665–671
Paper #178

FRICTIONLESS CONTACT OF ELASTIC BODIES: COMPARISON OF TREATMENT IN FINITE ELEMENT ANALYSI AND ISOGEOMETRIC ANALYSIS

J. Kopačka, R. Kolman, D. Gabriel, J. Plešek *

Abstract: *Artificial oscillations in contact force due to non-smooth contact surface are treated by isogeometric analysis (IGA). After brief overview of B-splines and Non-Uniform Rational B-Splines (NURBS) representation, the mortar-based contact algorithm is presented in the frictionless small deformation regime. Contact constraints are regularized by penalty method. The contact algorithm is tested by means of contact patch test.*

Keywords: ***Isogeometric analysis, Contact analysis, NURBS***

1. Introduction

The main difficulty in contact analysis is non-smoothness. It arises from inequality constraint as well as the geometric discontinuities inducted by spatial discretization. Contact analysis based on traditional finite elements utilizes element facets to describe a contact surface. The facets are C^0 continuous so that surface normal can experience jump across facet boundaries leading to artificial oscillations in contact force.

There were attempts to treat the geometric discontinuities by smoothing the contact surfaces using splines interpolation. These remedies introduce an additional geometry on the top of the existing finite element mesh. This adds an additional layer of data management and increasing computational overhead. Details and further references can be found in Wriggers (2006).

Another remedy to the geometric discontinuity provides isogeometric analysis (IGA). The fundamental idea is to accurately describe a physical domain of interest by proper representation (e.g. NURBS) and then utilize the same basis for analysis. This is in contrast with the classical finite element method where the basis is given in advance by the element type and so that the physical domain could be approximated inaccurately. More detailed description could be found in Cottrell et al. (2009).

Isogeometric NURBS-based contact analysis has some additional advantages: preserving geometric continuity, facilitating patch-wise contact search, supporting a variationally consistent formulation, and having a uniform data structure for the contact surface and the underlying volumes.

Geometric basis and formulation for frictionless isogeometric contact has been given in Lu (2010). Sharp corners or C^0 edges that can exist on the interface of patches present a challenge to contact detection. A strategy to seamlessly deal with sharp corners has been proposed in this reference. Herein, the contact constraints are regularized by penalty method and contact virtual work is discretized by finite strain surface-to-surface contact element. Both one-pass and two-pass algorithm are tested.

In Temizer et al. (2011), finite deformation frictionless quasi-static thermomechanical contact problems are considered. Two penalty-based contact algorithms are studied herein. The former is called knot-to-surface (KTS) algorithm. It is the straightforward extension of the classical node-to-surface (NTS) algorithm. Since NURBS control points are not interpolatory, contact constraints are enforce directly at the physical points of the quadrature points. It is shown in this reference that this approach is

*Ing. Ján Kopačka, Ing. Radek Kolman, Ph.D., Ing. Dušan Gabriel, Ph.D., Ing. Jiří Plešek, CSc.: Institute of Thermomechanics AS CR, v.v.i., Academy of Science of the Czech Republic, Dolejškova 1402/5; 182 00, Prague 8; CZ, e-mail: {kopacka,kolman,gabriel,plesek}@it.cas.cz

over-constrained and therefore not acceptable if a robust formulation with accurate tractions is desired. The latter is called mortar-KTS algorithm. In this algorithm a mortar projection to control pressures is employed to obtain the correct number of constraints.

The penalty-based mortar-KTS algorithm has been extended to frictional contact in Lorenzis et al. (2011) and Temizer et al. (2012). The mortar-KTS algorithm has been also studied in conjugation with augmented Lagrangian method in Lorenzis et al. (2012). Isogeometric frictionless contact analysis using non-conforming mortar method in two-dimensional linear elasticity regime has been presented in Kim (2011).

In this paper, we present mortar-based frictionless isogeometric contact algorithm in small deformation regime. The main contribution of this work is to prepare an implementation of the IGA procedures for further investigation. After brief overview of B-Splines and NURBS representation in section 2., the isogeometric contact algorithm is presented in section 3. The robustness of the algrithm is chacked by means of contact patch test in section 4.

2. B-splines and NURBS

This section gives a brief overview of the main concerns of B-splines and NURBS. For more detailed description as well as efficient algorithms see Piegl and Tiller (1997). Throughout this paper we use p to indicate the polynomial degree, n to indicate the number of basis functions, d_{p} to indicate the number of parametric dimensions, and d_{s} to indicate the number of spatial dimensions.

Let $\boldsymbol{\Xi}^i$, $i = 1, \dots d_{\mathrm{p}}$ be the open non-uniform knot vector associated with i^{th} parametric dimension of a patch

$$\boldsymbol{\Xi}^i \quad = \quad \left\{ \underbrace{\xi^i_1, \dots, \xi^i_{p_i+1}}_{p_i+1 \text{ equal terms}}, \xi^i_{p_i+2}, \dots, \xi^i_{n_i}, \underbrace{\xi^i_{n_i+1}, \dots, \xi^i_{n_i+p_i+1}}_{p_i+1 \text{ equal terms}} \right\}. \tag{1}$$

The knot vector is a non-decreasing sequence of parametric coordinates. The knot vector is said to be non-uniform if the knots are unequally spaced in the parametric space. If the first and the last knot value appears $p_i + 1$ times, the knot vector is called open. Open knot vectors are interpolatory at the corners of patches. It means that the boundary of a B-spline object with d_{p} parametric dimensions is itself a B-spline object of $d_{\mathrm{p}} - 1$.

The B-spline basis functions are defined by Cox-de Boor recursion formula. For $p = 0$

$$N_{j,0}(\xi) = \begin{cases} 1 & \xi \in [\xi_j, \xi_{j+1}), j = 1 \dots n \\ 0 & \text{otherwise,} \end{cases} \tag{2}$$

and for $p > 0$

$$N_{j,p}(\xi) = \frac{\xi - \xi_j}{\xi_{j+p} - \xi_j} N_{j,p-1}(\xi) + \frac{\xi_{j+1+p} - \xi}{\xi_{j+1+p} - \xi_{j+1}} N_{j+1,p-1}(\xi). \tag{3}$$

B-splines are known to be unable to exactly describe some curves, whereas rational functions can. NURBS (Non-Uniform Rational B-Splines) was developed to extend interpolatory capability of the B-splines. The extension originates from projection geometry of conic sections. A p^{th} degree NURBS basis function is defined by

$$R^p_j(\xi) = \frac{N_{j,p}(\xi) w_j}{\sum_{\hat{j}=1}^{n} N_{\hat{j},p}(\xi) w_{\hat{j}}}, \tag{4}$$

where w_j is referred to as the j^{th} weight.

Multivariate NURBS objects can be constructed simply by tensor product of univariate NURBS basis functions (4). For $d_{\mathrm{p}} = 2$

$$R^{p_1,p_2}_{j_1,j_2}(\xi^1, \xi^2) = R^{p_1}_{j_1}(\xi^1) \otimes R^{p_2}_{j_2}(\xi^2) = \frac{N_{j_1,p_1}(\xi^1) N_{j_2,p_2}(\xi^2) w_{j_1,j_2}}{\sum_{\hat{j}_1=1}^{n_1} \sum_{\hat{j}_2=1}^{n_2} N_{\hat{j}_1,p_1}(\xi^1) N_{\hat{j}_2,p_2}(\xi^2) w_{\hat{j}_1,\hat{j}_2}} \tag{5}$$

and similarly for the higher parametric dimension. With NURBS basis functions at hand we can finally introduce surface discretization by

$$\mathbf{x}(\xi^1,\xi^2)=\sum_{j_1=1}^{n_1}\sum_{j_2=1}^{n_2}R^{p_1,p_2}_{j_1,j_2}(\xi^1,\xi^2)\mathbf{P}_{j_1,j_2}, \tag{6}$$

where $\mathbf{P}_{j_1,j_2}\in\mathbb{R}^{d_\mathrm{s}}$ is the control net, i.e., array of coordinates of control points. Adopting the isogeometric concept, an analogous interpretation is used for unknown displacement field and its variation. Utilizing proper connectivity arrays according to Cottrell et al. (2009), one can write

$$\mathbf{x}(\boldsymbol{\xi})=\sum_{A=1}^{n_\mathrm{cp}}N_A(\boldsymbol{\xi})\mathbf{x}_A\qquad\mathbf{u}(\boldsymbol{\xi})=\sum_{A=1}^{n_\mathrm{cp}}N_A(\boldsymbol{\xi})\mathbf{u}_A\qquad\delta\mathbf{u}(\boldsymbol{\xi})=\sum_{A=1}^{n_\mathrm{cp}}N_A(\boldsymbol{\xi})\delta\mathbf{u}_A, \tag{7}$$

where $\boldsymbol{\xi}=(\xi^1,\xi^2)\in\mathbb{R}^{d_\mathrm{p}}$, A is the index of global basis function and n_cp is the number of control points. It is also useful to consider local mappings defined over one individual knot span which can be interpreted as a finite element

$$\mathbf{x}(\boldsymbol{\xi})=\sum_{a=1}^{n_\mathrm{ec}}N_a(\boldsymbol{\xi})\mathbf{x}_a\qquad\mathbf{u}(\boldsymbol{\xi})=\sum_{a=1}^{n_\mathrm{ec}}N_a(\boldsymbol{\xi})\mathbf{u}_a\qquad\delta\mathbf{u}(\boldsymbol{\xi})=\sum_{a=1}^{n_\mathrm{ec}}N_a(\boldsymbol{\xi})\delta\mathbf{u}_a, \tag{8}$$

where a is the number of local basis function, and n_ec is the number of element control points.

3. Isogeometric contact treatment

In this section we present isogeometric treatment of small displacement frictionless contact between two elastic deformable bodies. We adopt mortar-KTS algorithm according to Temizer et al. (2011) and customize it for the small displacement regime. For more detailed description of computational contact, the reader is referred to Wriggers (2006).

3.1. Contact kinematics

Consider two elastic bodies Ω_1 and Ω_2 in contact without friction. The size and the location of the contact boundary $\Gamma_\mathrm{c}=\partial\Omega_1\cap\partial\Omega_2$ is unknown. For its determination, a function which measures the distance between the bodies is introduced

$$d(\boldsymbol{\xi}):=\left\|\mathbf{x}_\mathrm{s}-\mathbf{x}_\mathrm{m}(\boldsymbol{\xi})\right\|,\quad\mathbf{x}_\mathrm{m}\in\partial\Omega_1,\,\mathbf{x}_\mathrm{s}\in\partial\Omega_2. \tag{9}$$

With the aid of this function one can assign to each slave point $\mathbf{x}_\mathrm{s}\in\partial\Omega_2$ a master point $\bar{\mathbf{x}}_\mathrm{m}\in\partial\Omega_1$ by the closest point projection

$$\boldsymbol{\nabla}d(\boldsymbol{\xi})=\frac{\partial\mathbf{x}_\mathrm{m}(\boldsymbol{\xi})}{\partial\boldsymbol{\xi}}\cdot\left[\mathbf{x}_\mathrm{s}-\bar{\mathbf{x}}_\mathrm{m}(\boldsymbol{\xi})\right]=\mathbf{0}. \tag{10}$$

This is a system of non-linear algebraic equations with respect to $\boldsymbol{\xi}=(\xi_1,\ldots,\xi_{d_\mathrm{p}})$. Different methods for its numerical solution were studied in Gabriel et al. (2011). Customizing to the isogeometric analysis is straightforward. It consists in replacing basis functions and its derivatives. The closest projection point as well as related variables will be indicated by the bar symbol further in this paper (e.g. $\bar{\mathbf{x}}_\mathrm{m}$, $\bar{\boldsymbol{\xi}}$).

With the closest point, $\bar{\mathbf{x}}_\mathrm{m}$, at hand we can define the normal gap as

$$g_\mathrm{N}=(\mathbf{x}_\mathrm{s}-\bar{\mathbf{x}}_\mathrm{m})\cdot\bar{\mathbf{n}}_\mathrm{m}=(\mathbf{u}_\mathrm{s}-\bar{\mathbf{u}}_\mathrm{m})\cdot\bar{\mathbf{n}}_\mathrm{m}+g_0, \tag{11}$$

and its variation

$$\delta g_\mathrm{N}=\left(\delta\mathbf{u}^1-\delta\bar{\mathbf{u}}^2\right)\cdot\bar{\mathbf{n}}_\mathrm{m}, \tag{12}$$

where $\mathbf{u}_\mathrm{s}$ and $\bar{\mathbf{u}}_\mathrm{m}$ are displacements of the slave and master points respectively, and g_0 is the initial normal gap.

3.2. Contact constraints

Non-penetration condition dictates that normal gap has to be non-negative. If the gap is closed, it has to generate pressure. These two natural criteria can be written as Karush-Kuhn-Tucker (KKT) condition for contact

$$g_{\mathrm{N}} \geq 0 \tag{13}$$

$$t_{\mathrm{N}} \leq 0 \quad \text{on } \Gamma_{\mathrm{c}}, \tag{14}$$

$$t_{\mathrm{N}} g_{\mathrm{N}} = 0 \tag{15}$$

where the third equality is called complementary condition. It states that either the gap or the contact traction has to be zero. One of the possibilities how to regularized the KKT conditions is the penalty method. The regularized normal contact constraint reads as

$$t_{\mathrm{N}} = \epsilon \langle g_{\mathrm{N}} \rangle , \quad \langle g_{\mathrm{N}} \rangle = \begin{cases} g_{\mathrm{N}} & \text{if } g_{\mathrm{N}} \leq 0 \\ 0 & \text{otherwise} \end{cases} , \tag{16}$$

where ϵ_{N} is the penalty parameter.

3.3. Weak form

Contact boundary value problem can be formulated in a weak sense by

$$\delta\Pi(\mathbf{u}, \delta\mathbf{u}) = \delta\Pi_{\mathrm{int}}(\mathbf{u}, \delta\mathbf{u}) + \delta\Pi_{\mathrm{ext}}(\mathbf{u}, \delta\mathbf{u}) + \delta\Pi_{\mathrm{c}}(\mathbf{u}, \delta\mathbf{u}) = 0, \tag{17}$$

subjected to (13). The terms on the right hand side denote virtual work due to internal forces, virtual work due to external forces and virtual work due to contact forces respectively. Assuming the validity of the action-reaction principle, contact virtual work can be expressed as

$$\delta\Pi_{\mathrm{c}}(\mathbf{u}, \delta\mathbf{u}) = \int_{\Gamma_{\mathrm{c}}} \epsilon_{\mathrm{N}} g_{\mathrm{N}} \delta g_{\mathrm{N}} \, \mathrm{d}\Gamma \tag{18}$$

3.4. Discretized form

By substituting (8) into (11) and (12), the normal gap and its variation becomes

$$g_{\mathrm{N}} = \left[\sum_{a=1}^{n_{\mathrm{ec}}^{\mathrm{s}}} R_a^{\mathrm{s}}(\boldsymbol{\xi}^{\mathrm{s}}) \mathbf{u}_a^{\mathrm{s}} - \sum_{a=1}^{n_{\mathrm{ec}}^{\mathrm{m}}} R_a^{\mathrm{m}}(\bar{\boldsymbol{\xi}}) \mathbf{u}_a^{\mathrm{m}} \right] \cdot \bar{\mathbf{n}}^{\mathrm{m}} + g_0(\bar{\boldsymbol{\xi}}), \tag{19}$$

$$\delta g_{\mathrm{N}} = \left(\sum_{a=1}^{n_{\mathrm{ec}}^{\mathrm{s}}} R_a^{\mathrm{s}}(\boldsymbol{\xi}^{\mathrm{s}}) \delta\mathbf{u}_a^{\mathrm{s}} - \sum_{a=1}^{n_{\mathrm{ec}}^{\mathrm{m}}} R_a^{\mathrm{m}}(\bar{\boldsymbol{\xi}}) \delta\mathbf{u}_a^{\mathrm{m}} \right) \cdot \bar{\mathbf{n}}^{\mathrm{m}}. \tag{20}$$

Defining the vectors

$$\mathbf{u} = \begin{bmatrix} u_1^{\mathrm{s}} \\ \vdots \\ u_{n_{\mathrm{ec}}^{\mathrm{s}}}^{\mathrm{s}} \\ u_1^{\mathrm{m}} \\ \vdots \\ u_{n_{\mathrm{ec}}^{\mathrm{m}}}^{\mathrm{m}} \end{bmatrix} \qquad \delta\mathbf{u} = \begin{bmatrix} \delta u_1^{\mathrm{s}} \\ \vdots \\ \delta u_{n_{\mathrm{ec}}^{\mathrm{s}}}^{\mathrm{s}} \\ \delta u_1^{\mathrm{m}} \\ \vdots \\ \delta u_{n_{\mathrm{ec}}^{\mathrm{m}}}^{\mathrm{m}} \end{bmatrix} \qquad \mathbf{N} = \begin{bmatrix} R_1^{\mathrm{s}}(\boldsymbol{\xi}^{\mathrm{s}}) \bar{\mathbf{n}}_{\mathrm{m}} \\ \vdots \\ R_{n_{\mathrm{ec}}^{\mathrm{s}}}^{\mathrm{s}}(\boldsymbol{\xi}^{\mathrm{s}}) \bar{\mathbf{n}}_{\mathrm{m}} \\ -R_1^{\mathrm{m}}(\bar{\boldsymbol{\xi}}) \bar{\mathbf{n}}_{\mathrm{m}} \\ \vdots \\ -R_{n_{\mathrm{ec}}^{\mathrm{m}}}^{\mathrm{m}}(\bar{\boldsymbol{\xi}}) \bar{\mathbf{n}}_{\mathrm{m}} \end{bmatrix}, \tag{21}$$

equations (19) and (20) can be cast in matrix form as

$$g_{\mathrm{N}} = \mathbf{N}^{\mathrm{T}} \mathbf{u} + g_0, \tag{22}$$

$$\delta g_{\mathrm{N}} = \delta\mathbf{u}^{\mathrm{T}} \mathbf{N}. \tag{23}$$

3.5. Mortar-KTS contact algorithm

In the spirit of the mortar method, the the contact virtual work is expressed as

$$\delta\Pi_{\mathrm{c}}(\mathbf{u},\delta\mathbf{u}) = \sum_{A} \epsilon_{\mathrm{N}} g_{\mathrm{N}_A} \delta g_{\mathrm{N}_A} A_A, \tag{24}$$

where summation is extended to the active control points. The control point normal gap and its variation are defined as the weighted average, with the basis functions as weights

$$g_{\mathrm{N}_A} = \frac{\int_{\Gamma_{\mathrm{c}}} R_A g_{\mathrm{N}} \,\mathrm{d}\Gamma}{\int_{\Gamma_{\mathrm{c}}} R_A \,\mathrm{d}\Gamma} \qquad \delta g_{\mathrm{N}_A} = \frac{\int_{\Gamma_{\mathrm{c}}} R_A \delta g_{\mathrm{N}} \,\mathrm{d}\Gamma}{\int_{\Gamma_{\mathrm{c}}} R_A \,\mathrm{d}\Gamma}. \tag{25}$$

An active control point is one for which $g_{\mathrm{N}A} \leq 0$. The 'area of competence' of a control point is defined as

$$A_A = \int_{\Gamma_{\mathrm{c}}} R_A \,\mathrm{d}\Gamma. \tag{26}$$

Substituting (25) and (26) into (24) yields

$$\delta\Pi_{\mathrm{c}} = \sum_{A} \frac{\epsilon_{\mathrm{N}}}{\int_{\Gamma_{\mathrm{c}}} R_A \,\mathrm{d}\Gamma} \int_{\Gamma_{\mathrm{c}}} R_A g_{\mathrm{N}} \,\mathrm{d}\Gamma \int_{\Gamma_{\mathrm{c}}} R_A \delta g_{\mathrm{N}} \,\mathrm{d}\Gamma. \tag{27}$$

Substituting (22) and (23) into (27)

$$\delta\Pi_{\mathrm{c}} = \delta\mathbf{u}^{\mathrm{T}} \sum_{A} \frac{\epsilon_{\mathrm{N}}}{\int_{\Gamma_{\mathrm{c}}} R_A \,\mathrm{d}\Gamma} \left(\int_{\Gamma_{\mathrm{c}}} R_A \mathbf{N} \,\mathrm{d}\Gamma \int_{\Gamma_{\mathrm{c}}} R_A \mathbf{N}^{\mathrm{T}} \,\mathrm{d}\Gamma \mathbf{u} + \int_{\Gamma_{\mathrm{c}}} R_A g_0 \,\mathrm{d}\Gamma \int_{\Gamma_{\mathrm{c}}} R_A \mathbf{N} \,\mathrm{d}\Gamma \right). \tag{28}$$

Finally, the contact residual vector is immediately obtained from (28)

$$\mathbf{G}_{\mathrm{c}} = \mathbf{K}_{\mathrm{c}} + \mathbf{F}_{\mathrm{c}}, \tag{29}$$

where by gauss integration

$$\mathbf{K}_{\mathrm{c}} = \sum_{A} \frac{\epsilon_{\mathrm{N}}}{\sum_{g=1}^{n_{\mathrm{gp}}} R_A(\boldsymbol{\xi}_g) w_g j_g} \sum_{g=1}^{n_{\mathrm{gp}}} R_A(\boldsymbol{\xi}_g) \mathbf{N} w_g j_g \sum_{g=1}^{n_{\mathrm{gp}}} R_A(\boldsymbol{\xi}_g) \mathbf{N}^{\mathrm{T}} w_g j_g, \tag{30}$$

$$\mathbf{F}_{\mathrm{c}} = \sum_{A} \frac{\epsilon_{\mathrm{N}}}{\sum_{g=1}^{n_{\mathrm{gp}}} R_A(\boldsymbol{\xi}_g) w_g j_g} \sum_{g=1}^{n_{\mathrm{gp}}} R_A(\boldsymbol{\xi}_g) g_0(\boldsymbol{\xi}_g) w_g j_g \sum_{g=1}^{n_{\mathrm{gp}}} R_A(\boldsymbol{\xi}_g) \mathbf{N} w_g j_g, \tag{31}$$

where w_g are Gauss-Legendre weights, j_g are the Jacobian determinant, both evaluated at Gaussian quadrature point $g = 1, \ldots, n_{\mathrm{gp}}$.

4. Contact patch test

In this section we present a three-dimensional version of the contact patch test acoording to Taylor and Papadopoulos (1991). Dimensions are depicted in the Fig. 1. Both blocks are subjected to a pressure $p = 1F/UL^2$. The same material with $\nu = 0.3$ and $E = 1000F/UL^2$ is used for both blocks. The analytical solution is $\sigma_z = -1F/UL^2$.

Either of the blocks is discretized by one trivariate NURBS patch of order $p = 1$ in each parametric dimension. The knot vectors are

$$\boldsymbol{\Xi}^i = \left\{ \begin{array}{cccccccc} 0 & 0 & 0.25 & 0.5 & 0.75 & 1 & 1 \end{array} \right\}, i = 1, \ldots, 3. \tag{32}$$

There are four nonzero knot spans which are depicted by the black grid in the Fig. 2. There are contours of the z-displacement field in the Fig. 2. The constant partial derivative with respect to z implies constant pressure in both blocks. The same results has been obtained for tri-quadratic and tri-cubic NURBS patches.

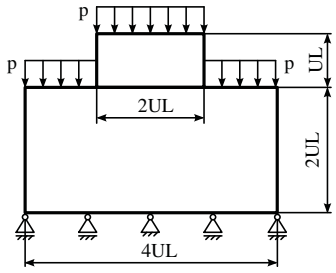

Fig. 1: The contact patch test according to Taylor and Papadopoulos (1991). UL is the unit length, $p = 1F/UL^2$ is the presuure.

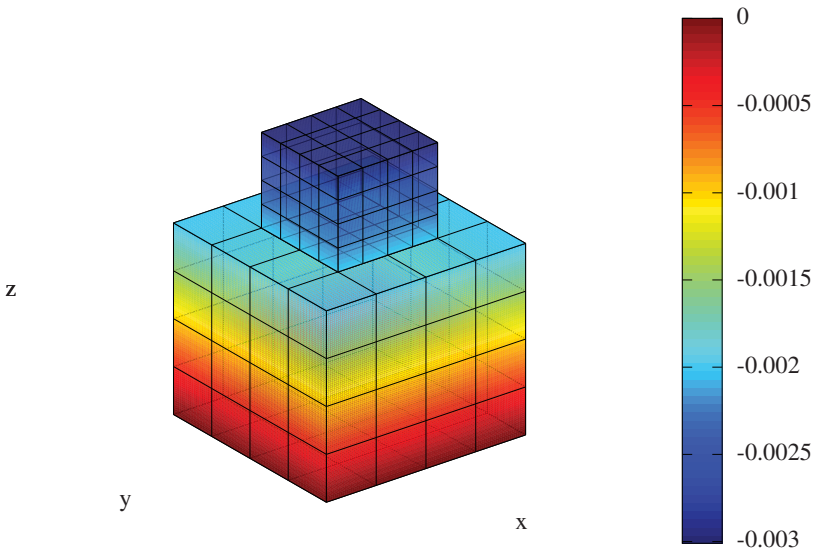

Fig. 2: Z-displacement field. The constant partial derivative with respect to z implies constant pressure.

5. Conclusions

The frictionless mortar-based isogeometric contact algorithm in small deformation regime has been outlined. The correct implementation of the contact algorithm has been successfully tested by means of contact patch test. Indeed, one cannot make serious conclusins based on one numerical example. Therefore, we will continue in the assessment of the algorithm in the further work.

Acknowledgements

This work was supported by the Grant Agency of the Czech Republic under grant numbers GAP101/12/2315, GPP101/10/P376, GA101/09/1630 in the framework of AV0Z20760514.

References

Wriggers, P. (2006), *Computational Contact Mechanics*, Springer, Berlin.

Cottrell, J.A., Hughes, T.J.R., Bazilevs, Y. (2009), *Isogeometric Analysis: Toward Integration of CAD and FEA*, John Wiley & Sons, New York.

Temizer, I., Wriggers, P., Hughes, T.J.R. (2011), Contact treatment in isogeometric analysis with NURBS. *Comput. Methods Appl. Mech. Engrg.*, Vol 200, pp 1100-1112.

Lu, J. (2010), Isogeometric contact analysis: Geometric basis and formulation for frictionless contact. *Comput. Methods Appl. Mech. Engrg.*, Vol 200, pp 726-741.

De Lorenzis, L., Temizer, I., Wriggers, P., Zavarise, G. (2011), A large deformation frictional contact formulation using NURBS-based isogeometric analysis. *Int. J. Numer. Meth. Engng.*, Vol 87, pp 1278-1300.

Kim, J.Y., - Youn, S.K. (2011), Isogeometric contact analysis using mortar method. *Int. J. Numer. Meth. Engng.*.

Temizer, I., Wriggers, P., Hughes, T.J.R. (2012) Three-dimensional mortar-based frictional contact treatment in isogeometric analysis with NURBS. *Comput. Methods Appl. Mech. Engrg.*, Vol 209-212, pp 115-128.

De Lorenzis, L., Wriggers, P., Zavarise, G. (2012) A mortar formulation for 3D large deformation contact using NURBS-based isogeometric analysis and the augmented Lagrangian method. *Comput. Mech.*, Vol 49, pp 1-20.

Piegl, L., Tiller, W. (1997) *The NURBS Book (Monographs in Visual Communication)*. Second Edition, Springer-Verlag.

Gabriel, D., Kopačka, J., Plešek, J., Ulbin, M. (2010), Assesment of methods for calculating the normal contact vector in local search. In: *In ECCM 2010*, Computational Structural Mechanics Association, Paris, 2 pp..

Taylor, R. L., Papadopoulos, P. (1991) On a patch test for contact problems in two dimensions. *Nonlinear Computational Mechanics*, pp 690-702, Springer, Berlin.